2014 IEEE International Conference on Robotics & Automation (ICRA)
Hong Kong Convention and Exhibition Center
May 31 - June 7, 2014. Hong Kong, China

Surface Normal Measurement in the End Effector of a Drilling Robot for Aviation

Peijiang Yuan, Qishen Wang, Tianmiao Wang, Chengkun Wang and Bo Song

***Abstract*-Aiming at the robot drilling perpendicularity in aircraft assembly, a surface normal measurement method is presented and a drilling end effector is designed. Four laser ranging sensors are uniformly distributed around the drill to measure the surface normal as four non-coplanar points define a unique circumscribed sphere and the sphere center can be calculated. By this principle, the method measures four points coordinates on the curved surface in the drilling area using four laser ranging sensors. If the four laser ranging sensors are close enough to each other, it is reasonable to assume that the drilling point is on the sphere surface. Therefore, the connection line of the sphere center and the drilling point is the surface normal at the drilling point. The angle θ between the normal and the axis of the drill is calculated and if θ is larger than 0.5 degree, the drilling end effector will adjust the attitude of the drill to make sure θ is smaller than 0.5 degree to meet the requirement in aircraft assembly. A novel adjusting mechanism is designed in the end effector which can keep drill vertex immobile when adjusting drill position. Thus, it is not required to remove the drill vertex to the mark point. Simulation results of three kinds curved surfaces show that the surface normal measurement method is accurate and efficient. Experiments on aviation drilling system results also demonstrate the adjusting mechanism is effective with high accuracy.**

I. INTRODUCTION

The service life of modern airplane has been improved increasingly and it can reach 5000 hours for main trunk airline[1]. It is reported that 70% fatigue failure accidents of airplane body are caused by joints position and 80% fatigue crack comes from riveting holes[2]. An experiment on Ti alloy indicates that the fatigue life of bolt will reduce 47% if the riveting holes are tilt beyond 2 degrees[3]. Therefore, the verticality of riveting holes has an extremely important effect on airplane life.

The verticality of a riveting hole depends on whether the normal at the drilling point coincides with the axis of the hole. Thus, surface normal measurement is a key technology in an aircraft automatic drilling system and the accuracy of measurement will greatly influence the verticality[4]. In recent years, many researchers have conducted a great deal of studies on the calculation method of surface normal. Megumi Saito measures a transparent curved surface normal by using polarization of light[5]. Hasegawa chooses a pair of wedge-prisms and a ranging sensor to obtain surface normal [6]. However, it is not suitable to measure normal by principles of optics in drilling robot system. Although quadratic surface fitting algorithm [7] possesses high precision in measuring surface normal on quadratic surface, but its accuracy is reduced when applied on the measurement of other surfaces and the selection of the measurement position should be optimized by a data reconciliation method which reduces the measurement efficiency. Gong et al. presents a three-point algorithm in which three laser ranging sensors are equispaced around a circle[8]. The normal is calculated from the cross product of any two vectors that are tangent to the surface at the drilling point. But the subpoint coordinate of drill vertex is difficult to measure in actual application. According to four non-coplanar points define a unique circumscribed sphere, Wang et al. proposes a algorithm of normal attitude regulation[9] which established a coordinate system at every laser ranging sensors and complicated coordinate transformation is needed. Besides, a reorientation algorithm is needed to remove the drill vertex to the drilling point as the design mechanism of his end effector.

After measuring the surface normal, an adjusting mechanism is needed in the end effector which can adjust the drill position to make the axis of drill coincide with the normal at drilling point. A robot drilling system with attitude adjusting module produced by the Electroimpact company has been applied in airplane assembly in Boeing company[10]. A 2-d.o.f. orientation device is designed by J.R.Serracín based on 2UPS−1U mechanism[11]. It can adjust the attitude of the scalpel and has applied in bone milling surgeries experiment. Using 2-DOFs rotation motions to rotate respectively along two axes which are perpendicular to each other, Wang et al. designs an end-effector for drilling robot[9]. However, it is needed to move the drill vertex to the drill position after adjusting the drill attitude. J. Antonio Briones designs a drilling robot based on CAPAMAN parallel mechanism and does experiments with the robot[12]. A 2R1T parallel mechanism is used by Shan et al. to realize adjusting the attitude of principal axis. Some drilling experiments have been done with the mechanism on butt joint of airplane wing body[13].

Compared with the above methods, the surface normal measurement algorithm is simple without complicated matrix transformation in different coordinate systems and the designed adjusting mechanism is novel which avoiding remove the drill vertex to the drilling point. The rest of this

The authors are with School of Mechanical Engineering & Automation, Beihang University, China. (Email: itr@buaa.edu.cn, wangqishen88@126.com, itm@buaa.edu.cn, wck179@163.com and jerrybo@sina.cn).

This research is partially supported by the National Natural Science Foundation of China (No.61075084 and No.61375085), Basic Research Fund of Center High School (No.303203) and Key Laboratory Fund of Beijing (No.Z131104002813099).

paper is organized as follows. Section II describes the principle and mechanism of normal measurement. Section III introduces the design of the drilling end effector, followed by the simulation, experimental results analysis in Section IV. Section V concludes the work.

II. NORMAL MEASUREMENT

A. Principle of normal measurement

Assuming four points in space are not co-planar, such as $A(x_A, y_A, z_A)$, $B(x_B, y_B, z_B)$, $C(x_C, y_C, z_C)$, and $D(x_D, y_D, z_D)$, and any three of them will determinate a unique circle. Without loss of generality, *A*, *B*, and *C* make the circle O_1 while *A*, *B*, and *D* make the circle O_2, as shown in Fig.1.

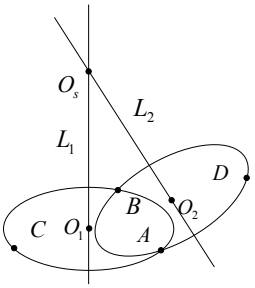

Fig.1 Four non-coplanar points define a unique circumscribed sphere O_s

Assuming the center coordinate of the circle O_1 is $(x_{O_1}, y_{O_1}, z_{O_1})$ and the radius of the circle O_1 is r_1. The equation of the plane which determined by the points *A*, *B*, and *C* can be expressed as

$$\begin{vmatrix} x & y & z & 1 \\ x_A & y_A & z_A & 1 \\ x_B & y_B & z_B & 1 \\ x_C & y_C & z_C & 1 \end{vmatrix} = 0 \tag{1}$$

Equation (1) can be transformed as

$$A_1 x + B_1 y + C_1 z + D_1 = 0 \tag{2}$$

where

$$\begin{aligned} A_1 &= y_A \cdot z_B - y_A \cdot z_C - y_B \cdot z_A \\ &\quad + y_C \cdot z_A + y_B \cdot z_C - y_C \cdot z_B \\ B_1 &= -x_A \cdot z_B + x_A \cdot z_C + x_B \cdot z_A \\ &\quad - x_C \cdot z_A - x_B \cdot z_C + x_C \cdot z_B \\ C_1 &= x_A \cdot y_B - x_A \cdot y_C - x_B \cdot y_A \\ &\quad + x_C \cdot y_A + x_B \cdot y_C - x_C \cdot y_B \\ D_1 &= -x_A \cdot y_B \cdot z_C + x_A \cdot y_C \cdot z_B + x_B \cdot y_A \cdot z_C \\ &\quad - x_C \cdot y_A \cdot z_B - x_B \cdot y_C \cdot z_A + x_C \cdot y_B \cdot z_A \end{aligned}$$

As the distances between O_1 and *A*, *B*, and *C* are all r_1:

$$(x_A - x_{O_1})^2 + (y_A - y_{O_1})^2 + (z_A - z_{O_1})^2 = r_1^2 \tag{3}$$

$$(x_B - x_{O_1})^2 + (y_B - y_{O_1})^2 + (z_B - z_{O_1})^2 = r_1^2 \tag{4}$$

$$(x_C - x_{O_1})^2 + (y_C - y_{O_1})^2 + (z_C - z_{O_1})^2 = r_1^2 \tag{5}$$

Combine the left part of (3) and (4), (3) and (5) respectively

$$A_2 x + B_2 y + C_2 z + D_2 = 0 \tag{6}$$

$$A_3 x + B_3 y + C_3 z + D_3 = 0 \tag{7}$$

where

$$\begin{aligned} A_i &= 2(x_j - x_{O1}) \\ B_i &= 2(y_j - y_{O1}) \\ C_i &= 2(z_j - z_{O1}) \\ D_i &= x_{O1}^2 + y_{O1}^2 + z_{O1}^2 - x_j^2 - y_j^2 - z_j^2 \end{aligned} \tag{8}$$

(if i=2 then j=*B*, else i=3 then j=*C*)

Rewrite (2)(6)(7) in matrix form

$$\begin{bmatrix} A_1 & B_1 & C_1 \\ A_2 & B_2 & C_2 \\ A_3 & B_3 & C_3 \end{bmatrix} \begin{bmatrix} x \\ y \\ z \end{bmatrix} + \begin{bmatrix} D_1 \\ D_2 \\ D_3 \end{bmatrix} = 0 \tag{9}$$

Thus, the coordinate of circle center O_1 can be expressed as

$$\begin{bmatrix} x_{O_1} \\ y_{O_1} \\ z_{O_1} \end{bmatrix} = -\begin{bmatrix} A_1 & B_1 & C_1 \\ A_2 & B_2 & C_2 \\ A_3 & B_3 & C_3 \end{bmatrix}^{-1} \begin{bmatrix} D_1 \\ D_2 \\ D_3 \end{bmatrix} \tag{10}$$

Meanwhile, the vertical L_1 of circle O_1 through O_1 point is

$$\frac{x - x_{O_1}}{A_1} = \frac{y - y_{O_1}}{B_1} = \frac{z - z_{O_1}}{C_1} \tag{11}$$

In the same way, we can get the vertical L_2 of circle O_2 through O_2 point

$$\frac{x - x_{O_2}}{A_1'} = \frac{y - y_{O_2}}{B_1'} = \frac{z - z_{O_2}}{C_1'} \tag{12}$$

According to the knowledge of geometry, the center of the sphere is the point of intersection of L_1 and L_2.Therefore, from (11) and (12),we can obtain the coordinate $O_s(x_s y_s z_s)$ of the sphere center. So four points which are not co-plane arbitrarily in space can determine a sphere and its center coordinate can be calculated.

Assuming a drill position coordinate $M(x_m, y_m, z_m)$ on the workpiece surface, it can be accepted that $M(x_m, y_m, z_m)$ is on the sphere which is circumscribed with *A*, *B*, *C*, and *D* when the four points are close to each other. Thus, vector quantity $\boldsymbol{O_sM}$ is the normal at *M* point and the calculation flow is shown in Fig.2.

B. Mechanism of normal measurement

Four laser ranging sensors are equispaced on a circle which the radius is r_0 and make the emitting laser points L_1, L_2, L_3, and L_4 on the circle, as shown in Fig.3.When the end effector moves close to the workpiece, the laser ranging sensors emit laser and measure the distance between the emitting points and their subpoints on the workpiece. O-xyz coordinate system is established in which OL_1 is *x* axis and OL_2 is *y* axis. Then the coordinates of *A*, *B*, *C*, and *D* can be

wrote as $A(r_0,0,-d_1)$, $B(0,r_0,-d_2)$, $C(-r_0,0,-d_3)$, and $D(0,-r_0,-d_4)$.

According to the measure surface normal principle, we can calculate the $O_s(x_s,y_s,z_s)$.

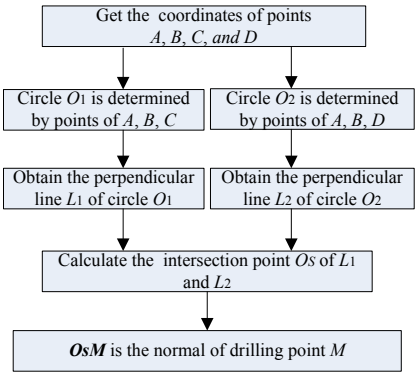

Fig.2 Calculation flow for the normal

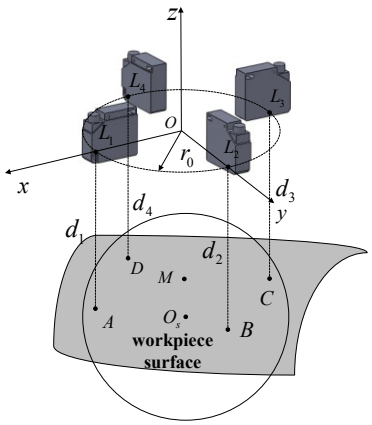

Fig.3 Mechanism of normal measurement

An intelligent Cognex camera is used to measure the drilling position $M(x_{cam},y_{cam},z_{cam})$ at the camera coordinate system. We can get the $M(x_m,y_m,z_m)$ at the O-xyz coordinate system through transformation of coordinates.The normal at M can be expressed as

$$\boldsymbol{O_sM}=(x_m-x_s,y_m-y_s,z_m-z_s) \tag{13}$$

The unit normal vector is

$$\begin{aligned}\boldsymbol{e}&=[e_x\ e_y\ e_z]^{\mathrm{T}}\\&=\frac{[x_m-x_s\ y_m-y_s\ z_m-z_s]^{\mathrm{T}}}{\sqrt{(x_m-x_s)^2+(y_m-y_s)^2+(z_m-z_s)^2}}\end{aligned} \tag{14}$$

III. Drilling End Effector

Drilling end effector is a key component of the robot drilling system. As the accuracy of industry robot can not meet the requirement in aircraft assembly[14], an adjusting mechanism is needed in the end effector to adjust the attitude of drill.

As shown in Fig.4, the end effector consists of the Spindle & the Feed Unit(SFU), the Vision Location Unit(VLU), the Adjusting Attitude Unit(AAU), the Scrap Absorption & the Press Unit(SAPU), the Normal Measurement Unit(NMU). The position of the drilling mark point is orientated by VLU and then the normal at the drilling point is measured by NMU. The angle θ between the normal and the axis of drill will be calculated and if θ does not meet the requirement in aircraft assembly, that is θ<0.5 degree, the attitude of drill will be adjusted by AAU. Finally, the SAPU press on the workpiece to prevent the vibration during drilling and the SFU start to drill. The SAPU will absorb the drill chippings to avoid they scratch the holes. The working flow is shown in Fig.5.

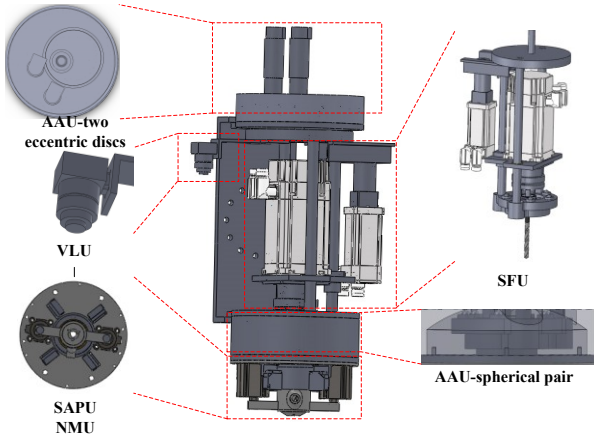

Fig.4 The drilling end effector

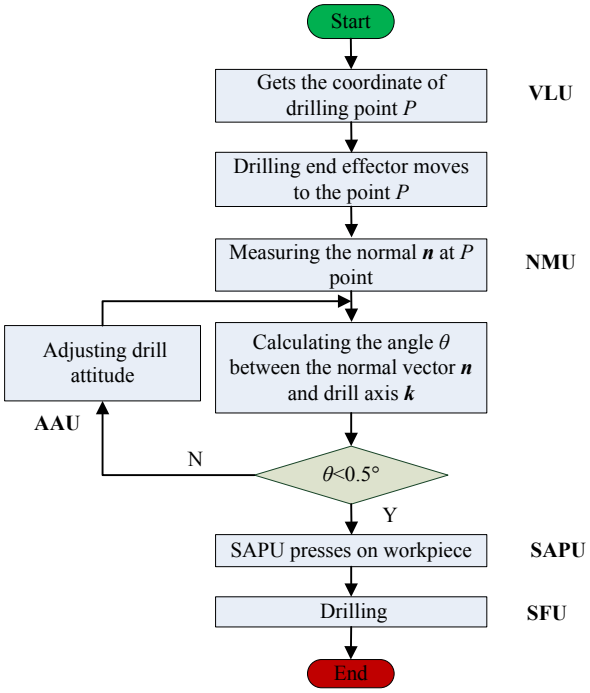

Fig.5 Working flow of drilling

In AAU, an adjusting mechanism is designed which includes two eccentric discs and a spherical pair. The draft of the mechanism is shown in Fig.6. There are two rotundity eccentric discs in the mechanism and both radii of the eccentric discs are r. The geometry axis of the small eccentric

disc coincides with the eccentric axis of big eccentric disc, as O_1 line shown in Fig.6. O line is the geometry axis of big eccentric disc and O_2 line is the eccentric axis of the small eccentric disc. A spherical plain bearing is mounted at the eccentric axis of the small eccentric disc and the axis of drill across the spherical hinge. The drill vertex locates at the center of sphericalpair, that is O_{sp} point. When the two eccentric discs rotate a full circle, the swept area of the axis of drill is a taper, as shown in Fig.7. That is, when the two eccentric discs rotate different angles, the axis of drill can reach an arbitrarily position in the taper and the progress is an adjusting attitude of the drill axis. As the drill vertex is located at the center of the spherical pair center, during the adjusting progress, the drill vertex is static which can avoid removing the drill vertex to drill position and this is an immense advantage compared with other end effectors which are presented in [9][15] which need a reposition progress after adjusting the drill attitude.

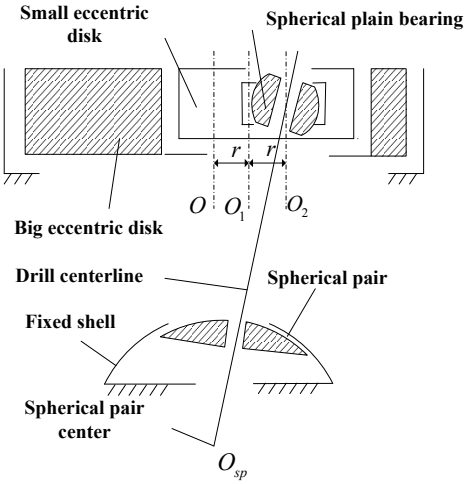

Fig.6 Draft of adjusting mechanism

As shown in Fig.7, the maximal adjusting angle φ can be expressed as

$$\varphi = \arctan(\frac{2r}{d}) \tag{15}$$

where d is the distance between the drill top point O and adjusting plane π.

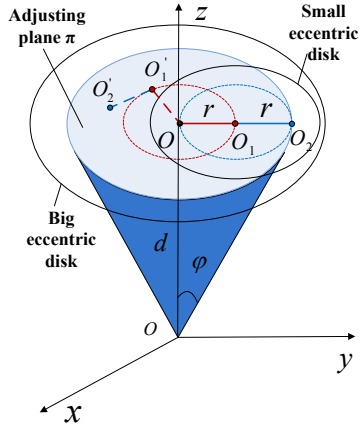

Fig.7 The scope of drill axis

So the adjusting angle scope is [0, φ]. In the designed end effector, r=25mm and d=570mm. Thus, $\varphi = \arctan(\frac{2*25}{570}) = 5^\circ$, that is the adjusting mechanism can adjust drill attitude in 5 degrees.

IV. Simulation and Experiment

A. Simulation

In simulation, three kinds of curved surface, expressed as $F(x,y,z)$, are used to prove the surface normal measurement method. Point $M(x_m, y_m, z_m)$ on the curve is the drilling point. The theoretical normal $\boldsymbol{n}_r$ at point M can be obtained from the following equation.

$$\boldsymbol{n}_r = [\frac{\partial F}{\partial x}, \frac{\partial F}{\partial y}, \frac{\partial F}{\partial z}]\Big|_{(M)} \tag{16}$$

Four points which are not co-plane are selected to calculate the normal $\boldsymbol{n}_m$ at point M using the method in part III. Then the angle θ between $\boldsymbol{n}_r$ and $\boldsymbol{n}_m$ is calculated. If θ meets the requirement of the airplane assembly, that is $\theta < 0.5^\circ$, the four points measure normal is proved viable.

The first equation of an ellipsoid surface for simulation is expressed as

$$\frac{x^2}{25} + \frac{y^2}{9} + \frac{z^2}{9} = 1 \tag{17}$$

As shown in Fig.8(a), the theoretical normal $\boldsymbol{n}_r$ at point M is calculated in MATLAB by using (16).

The second equation of a paraboloid surface for simulation is

$$3x^2 + y^2 - z = 0 \tag{18}$$

In the same way, the theoretical normal $\boldsymbol{n}_r$ at point M is shown in Fig.8(b).

The third equation of a cylndrical surface for simulation is

$$\begin{cases} x^2 + y^2 = 4 \\ z \subset R \end{cases} \tag{19}$$

In the same way, the theoretical normal $\boldsymbol{n}_r$ at point M is shown in Fig.8(c).

As the measurement normal $\boldsymbol{n}_m$ nearly coincides with theoretical normal $\boldsymbol{n}_r$, the $\boldsymbol{n}_m$ are not marked in Fig. 8 to show the $\boldsymbol{n}_r$ clearly.

TABLE I shows $\boldsymbol{n}_r$, $\boldsymbol{n}_m$ and θ at some selected points M in which marks 1-4 are on the ellipsoid surface expressed by (17), 5-8 are on the paraboloid surface expressed by (18) and 9-12 are on the cylndrical surface expressed by (19).

From TABLE I, it can be found that $\theta < 0.5^\circ$ at all selected points, which means the normal algorithm using four non-coplanar points is effective to meet the perpendicularity requirement of holes in aircraft assembly.

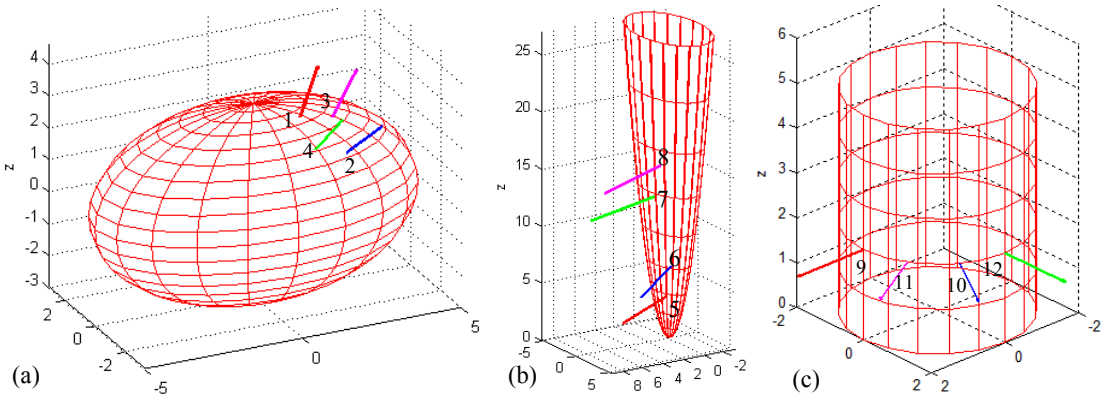

Fig.8 The theoretical normal at *M* point on: (a) ellipsoid surface (b) paraboloid surface (c) cylndrical surface

TABLE I Simulation data of proving the normal measurement method

	M	$\boldsymbol{n}_r$	$\boldsymbol{n}_m$	θ /°
1	(1, −1, 2.7641)	(0.0800, −0.2222, 0.6124)	(0.2955, −0.8232, 2.2745)	0.0190
2	(2, −2, 1.8868)	(0.1600, −0.4444, 0.4193)	(42.5964, −119.0640, 111.0674)	0.3152
3	(2, −1, 2.5612)	(0.1600, −0.2222, 0.5692)	(1.0261, −1.4232, 3.6453)	0.0192
4	(1, −2, 2.1541)	(0.0800, −0.4444, 0.4787)	(0.3727, −2.0667, 2.2272)	0.0168
5	(1, 1, 4)	(6, 2, −1)	(−3.0248, −1.0082, 0.5038)	0.0066
6	(1, 2, 7)	(6, 4, −1)	(−2.8219, −1.8847, 0.4696)	0.0505
7	(2, 1, 13)	(12, 2, −1)	(−6.0530, −1.0077, 0.5064)	0.0213
8	(2, 2, 16)	(12, 4, −1)	(−5.5509, −1.8522, 0.4593)	0.0368
9	(2, 0, 2)	(4, 0, 0)	(1.9717, 0.0023, 0.0017)	0.0831
10	(1, 1.7321, 2)	(2, 3.4641, 0)	(0.2403, 0.4171, 0.0008)	0.1089
11	(1.7321, 1, 2)	(3.4641, 2, 0)	(1.2753, 0.7377, 0.0010)	0.0612
12	(0, 2, 2)	(0, 4, 0)	(0.0016, 1.9853, 0.0026)	0.0881

A. Experimental result

The drilling end effector is mounted on the experimental platform of aviation drilling robot, as shown in Fig. 9. The aviation drilling robot comprises the base body, the suckers, the drilling end effector and the control system. The base body bears the weight of the drilling end effector and the drilling end effector can move on the base body with two directions. The suckers are adsorbed on the workpiece surface. The drilling function is completed by the drilling end effector, and the Austria B&R controller is used in the control system.

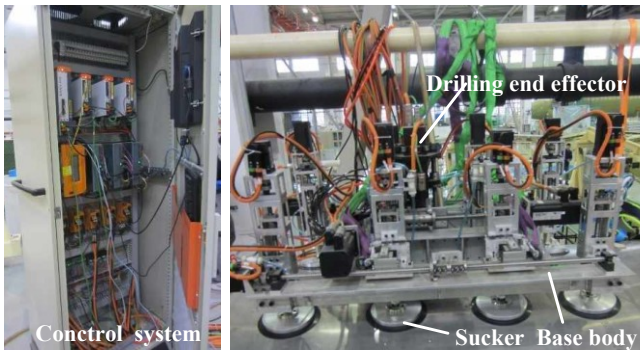

Fig.9 The aviation robot drilling system

In the experiment, the drilling end effector scans the mark point on the workpiece surface, when the mark point is determined, the end effector moves on the base body until the drill vertex is above the mark point.Then, four laser ranging sensors emit laser to the surface to obtain four projection points on the surface, as shown in Fig.10. The measurement normal $\boldsymbol{n}_m$ of mark point *M* is calculated by four points measurement method, and the connection line between drill vertex and spherical hinge center is the drill centerline direction, then we can get the direction of unit vector $\boldsymbol{n}_d$ from (14). Adjusting mechanism is driven by attitude adjustment motors to adjust the attitude of drill, until the angle θ between $\boldsymbol{n}_d$ and $\boldsymbol{n}_m$ reaches the requirement of hole vertical in aircraft assembly, that is $\theta < 0.5^\circ$ .The measurement data are shown in TABLE II.

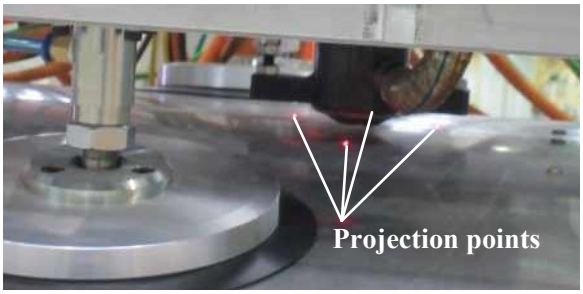

Fig.10 Laser sensors emit laser to workpiece surface

TABLE II Experiment data of drilling

	M	$\boldsymbol{n}_d$	$\boldsymbol{n}_m$	θ /°
Al	(0, 0, −85.5256)	(0.1219, −0.3385, 0.9330)	(0.2955, −0.8232, 2.2745)	0.0578
Ti	(0, 0, −85.9653)	(0.2533, −0.3518, 0.9012)	(1.0261, −1.4232, 3.6453)	0.0207
CFRP	(0, 0, −85.6834)	(0.1216, −0.6753, 0.7274)	(0.3727, −2.0667, 2.2272)	0.0159

Drilling experiments were fulfilled on aluminium alloy, titanium alloy and carbon fibre composite(CFRP) respectively. As shown in TABLE II, the angle θ between $\boldsymbol{n}_m$ and $\boldsymbol{n}_d$ are all meet for the requirement of holes vertical in aircraft assembly. Fig. 11 shows the comparison of the effect of drilling. (a) displays the drilling effect by an end effector without attitude adjustment mechanism while (b)

demonstrates the effect with adjusting mechanism. Comparing (a) with (b), take the holes drilled on Al for example, the diameters of the two holes are measured at intervals of 30 degrees and the diameters' profile of the holes are shown in Fig. 12.

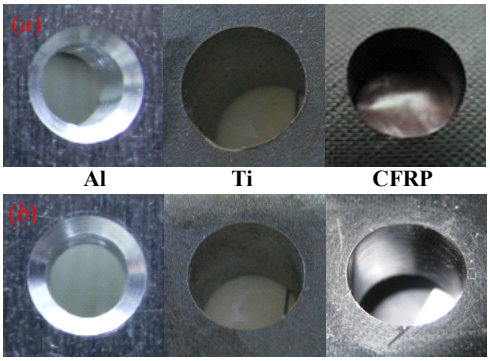

Fig.11 The effect of adjusting drill attitude

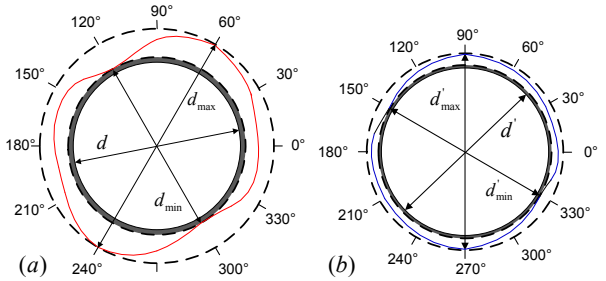

Fig.12 The diameters' profile of the holes

In Fig. 12(a), the maximum diameter $d_{\max} = 5.068mm$ and the minimum diameter $d_{\min} = 5.011mm$ .Therefore, the roundness $\Delta d = 0.057mm$. While in (b), $d'_{\max} = 5.015mm$, $d'_{\min} = 5.010mm$ and $\Delta d' = 0.005mm$. The results indicate that the roundness of the hole drilled by the designed end-effector with attitude mechanism is far smaller than that of the hole drilled by end-effector without attitude mechanism. The smaller the roundness is, the smaller the perpendicularity is. Thus, it can be proved indirectly that the surface normal measurement and the double eccentric discs adjusting mechanism can prove the perpendicularity of holes.

V. Conclusion

In this paper, a novel method for surface normal measurement and an original design for adjusting drill attitude in robot drilling end effector are presented. The normal at drilling point is measured by four laser ranging sensors which are equispaced on a circle. Simulation results show the measurement method for surface normal possesses a high accuracy. The characteristic of the adjusting mechanism is that it can make drill vertex keep static during adjusting attitude of the drill. As the original design for adjusting mechanism, the drilling efficiency will be increased because this mechanism can avoid removing drill vertex to the drilling position after adjusting the attitude of the drill. Experiments on aluminium alloy, titanium alloy and carbon fibre composite are implemented by a climbing robot drilling system. The results indicate that the method for surface normal measurement and the adjusting mechanism are effective to improve the verticality of holes in aircraft assembly.

Acknowledgment

The authors would like to thank National Natural Science Foundation of China, Commercial Aircraft Corporation of China, Ltd. and Beijing Municipal Science & Technology Commission sincerely for their support to this project. Besides, the participants in this research are all thankworthy for their contribution to the research.

References

[1] S. Davies, "UAVs in the firing line," *Engineering & Technology*, vol. 6, no. 8, pp. 34–36, Sep. 2011.

[2] L. Wang, and T. Feng, "Application of Digital Automatic Drill-Riveting Technology in Aircraft Manufacture," *Aeronautical Manufacturing Technology*, no. 11, pp. 42–45, Jun. 2008.

[3] G. Cao, "Research on Industry Robot Precision Drilling," M.S. thesis, Dept. Mech. Eng., Zhejiang Univ., Zhejiang, China, 2012.

[4] C. Proppe, "Probabilistic analysis of multi-site damage in aircraft fuselages," *Computational Mechanics*, vol. 30, no. 4, pp. 323–329, Mar. 2003.

[5] M. Saito, Y. Sato, K. Ikeuchi, and H. Kashiwagi, "Measurement of Surface Orientations of Transparent Objects Using Polarization in Highlight," *JOSA A*, vol. 16, no. 9, pp. 2286–2293, Sep. 1999.

[6] N. Hasegawa, T. Okada, and T. Shimizu, "Measurement of Surface Normal Using a Range Sensor with a Pair of Wedge-Prisms," in *2005 International Conference on Instrumentation and Measurement Technology, IMTC*, Ottawa, Canada, 2005, pp. 1744–1749.

[7] G. Ying, Z. Wang, Y. Kang, Z. Wu, and Z. Hu, "Study on Normal Vector Measurement Method in Auto-drilling and Riveting of Air-craft Panel," *Machine Tool and Hydraulics*, vol. 38, no. 20, pp. 1–8, Dec. 2010.

[8] M. Gong, P. Yuan, T. Wang, L. Yu, H. Xing, and W. Huang, "A novel method of surface-normal measurement in robotic drilling for aircraft fuselage using three laser range sensors," in *Advanced Intelligent Mechatronics (AIM), 2012 IEEE/ASME Int. Conf. on. IEEE,* 2012, pp. 450–455.

[9] L. Zhang, and X. Wang, "A novel algorithm of normal attitude regulation for the designed end-effector of a flexible drilling robot," *Journal of Southeast University (English Edition)*, vol. 28, no. 1, pp. 29–34, Mar. 2012.

[10] Russell DeVlieg. Robotic Trailing Edge Flap Drilling System[J]. SAE2009 AeroTech Congress & Exhibition. SAE Technical Papers. 2009: 01-3244.

[11] J.R. Serracína, L.J. Puglisib, R. Saltarenb, G. Ejarqueb, J.M. Sabater-Navarroc, and R. Aracilb, "Kinematic analysis of a novel 2-d.o.f. orientation device," *Robotics and Autonomous Systems*, vol. 60, no. 6, pp. 852–861, Jun. 2012.

[12] J. A. Briones, E. Castillo, G. Carbone, and M. Ceccarelli, "Position and Force Control of a Parallel Robot Capaman 2 Bis Parallel Robot for Drilling Tasks," in *Electronics, Robotics and Automotive Mechanics Conference*, Cuernavaca, Morelos, Mexico, 2009, pp. 181–186.

[13] Y. Shan, N. He, L. Li, Y. Yang, X. Qin, and W. Fang,"Spindle's prompt normal posture alignment method for assembly holemaking on large suspended panel," *Mechanical Science and Technology for Aerospace Engineering*, vol. 11, no. 30, pp. 1844–1849, Nov. 2011.

[14] H. Kihlman, G. Ossbahr, M. Engström, and J. Anderson, "Low-cost Automation for Aircraft Assembly," in *Proceedings of the Aerospace Manufacturing and Automated Fastening Conference*, St. Louis, MO, USA, 2004, pp. 117–124.

[15] M. Gong, P. Yuan, T. Wang, and R. Zhang, "Intelligent verticality-adjustment method of end-effector in aeronautical drilling robot," *Journal of Beijing University of Aeronautics and Astronautics*, vol. 38, no. 10, pp. 1400–1404, Oct. 2012.